ACS OMEGA

http://pubs.acs.org/journal/acsodf

Article

Influence of Areca Nutshell-Reduced Graphene Oxide, Isopropanol, and Exhaust Gas Recirculation in an Internal Combustion Engine

Kandasamy Muralidharan, Ganapathi Arumugam,* Amjad A. Pasha, and Nazrul Islam

Cite This: *ACS Omega* 2022, 7, 40815−40825

Read Online

ACCESS | Metrics & More | Article Recommendations

ABSTRACT: Regulations governing pollution, declining fossil fuel supply, and technological breakthroughs in renewable fuels all have a profound influence on the development of alternative fuels. This current research focuses on the influence of nanoadditives with alcohol in an exhaust gas recirculation-cooled engine. As nanoadditives have high thermal conductivity and alcohol has high oxygen content, they work synergistically to speed up the catalytic process and increase the combustion rate. The areca nutshell-reduced graphene oxide with a mass fraction of 25 pmm was ultrasonically blended with two isopropanol−diesel mixtures 10% isopropanol + 90% diesel (IDR10) and 20% isopropanol + 80% diesel (IDR20), respectively, and tested in a single-cylinder, 4-stroke internal-combustion engine at a typical injection timing of 23° TDC with an EGR rate of 20%. The results of experiments showed that IDR10 has better combustion and emission parameters than other fuel blends. Compared to other biodiesel blends, the IDR10 blend has 2.3% less BSFC and 2.45% more BTE. The IDR10 blend has lower HC emissions by 42.85%, CO emissions by 33.34%, NO_x emissions by 2.42%, and smoke emissions by 15.4%.

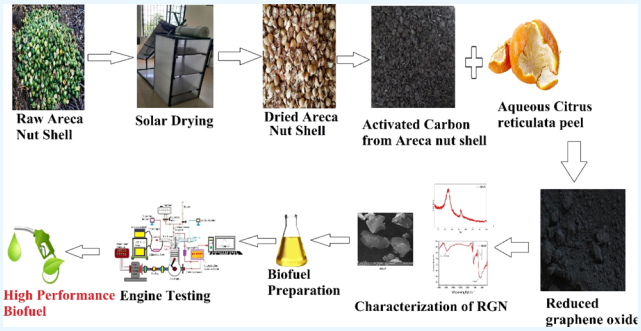

1. INTRODUCTION

15 billion vehicles are in use every day in the current decade, mostly due to urban industrialization and a rapidly increasing global population.[1] Because of this, the main difficulty faced around the globe is developing an alternative fuel, which needs to meet a variety of requirements, including depleting fossil resources and the need to give energy to society. Alcohols like isomers of propanol and butanol are attractive because of their favorable physical and chemical characteristics.[2]

Isopropyl alcohol has been used as a substitute in a variety of studies.[3] It was discovered that enhancing the concentrations of *n*-heptane−isopropanol in a homogeneous charge compression ignition engine decreases both the cylinder pressure and the volume of heat released.[4] When isopropanol is mixed with diesel, it has a longer delay time, less NO_x and CO_2 emissions, and a faster combustion rate.[5]

Nanomaterials improve the properties of biofuel blends (such as viscosity and flash) due to their huge surface area, weight diffusivity, and thermal heat transfer.[6] Fuel blends using nanoparticles may reduce carbon emissions by serving as catalysts. Metal oxide nanomaterials, such as aluminum, cerium, titanate, ferric oxide, and others, are quite common.[7] The addition of alcohol (diethyl ether) and nanoadditives considerably decreased the formation of NO_x, HC, CO, and soot by 31, 18, 33, and 11%, respectively.[8] Exhaust gas recirculation (EGR) and nanoadditives enhance fuel efficiency while reducing hazardous emissions. However, nanoparticles made of metal oxides would be toxic for health. Thus, bio-based nanoparticles, which counter this effect, are part of many modern research studies. In this investigation, based on the previous experimental investigations,[9] unique and high-reactive graphene oxide nanoplatelets (RGN) were preferred due to their better conductivity with one-atom thinness and SP^2 hybridization with a hexagonal structure configuration.[10]

EGR, an effective, versatile, and dependable emission reduction technology, may be used to reduce NO_x emissions.[10] For increased EGR proportions, the specific heat rises due to recycled CO_2 and H_2O, which have a greater specific heat value than O_2 and N_2. This decreases the pressure of the cylinder.[11] As a consequence of the lower intake of O_2 proportion, the flames spread farther, lowering the local temperature, and also due to increased EGR levels, soot production is limited. The "chemical influence", "thermal influence", and "dilution influence" are the three main characteristics of EGR.[12] Differences between these phenomena are mostly due to the localized substitution of inflow

Received: June 2, 2022
Accepted: October 26, 2022
Published: November 4, 2022

Figure 1. Making of areca nutshell charcoal.

Figure 2. Synthesis of RGN.

charge by inert gases, which results in the reduction of O_2 concentration. This soothes the flame, reducing the amount of NO_x produced.[13]

The areca nut tree, a member of the Arecaceae family, is a salt-resistant perennial tree that is found growing in a range of locales, including southern India, Tibet, Indonesia, Malaysia, and Burma. Corals of areca nutshells contain an inedible substance and a compostable fiber. The nutshell's sponginess increases with age, the green hue fades, and the fibers become coarser. Nonetheless, unmanaged nutshells emit foul smells and hinder waste removal following harvest. The waste-to-resource idea is needed to properly start managing feedstocks, including areca nutshells. A result of this is that the end product may well be reused effectively if areca nutshell waste is turned into nanoparticles.[14]

Chemical synthesis of reduced graphene oxide (RGO) involves hazardous chemicals. To eliminate this drawback, bio-based extracts are used in the synthesis process. Among the many bio-based extracts, aqueous *Citrus reticulata* peel has higher polyphenol concentration, which makes it a suitable antioxidant for the RGO preparation process.[15]

1.1. Novelty and Innovation of Present Study. All the above studies focused only on analyzing the performance, combustion, and emission characteristics powered by metal-based nanoadditives, except a few literature studies focusing on the availability of bio-waste as nanomaterials and its generic applications. Therefore, the proposed work aims one to develop a novel systematic methodology for the implementation of bio-based areca nutshell waste as nanoparticles along with isopropanol as biofuel for the partial replacement of diesel fuel in CI engines. To further reduce NO_x emissions, the use of an engine-cooled EGR system, which recycles exhaust gas at a volume ratio of 20%, is added. Within this context, the present work focuses on the investigation of the performance, combustion, and emission characteristics of blending with alcohol (isopropanol at 10 and 20%) along with bio-based nanoadditives (25 ppm of RGN) and operating in an engine-cooled EGR setup recirculating exhaust gas at a volume proportion of 20%.

2. EXPERIMENTAL ANALYSIS

2.1. Making of Areca Nutshell Charcoal. After purchasing the areca nutshell from a local trader (Dinesh, Vallapadi, Tamilnadu, India), all undesired components were removed. After washing and cleaning, the areca nut shell was dried in a sun dryer for 5 days. A kilogram of dried areca nutshell was carbonized for 6 h at 600 °C. The carbonized nutshell was crushed and sieved to a 50 μm powder. This is illustrated in Figure 1.

2.2. Synthesis of GO from Areca Nutshell Charcoal. For 30 min, H_2SO_4 (250 mL) was agitated in an ice bath environment with 10 g of graphite-based areca nutshell charcoal and 5 g of $NaNO_3$. The color of the solution changed to a dark green when it was stirred for 3 h at 20 °C in an ice bath after adding 3 g of $KMnO_4$. Afterward, the sample was taken out of an ice bath and stirred for a further 60 min at 35 °C. Then, 100 mL of deionized water was gradually introduced into the mixture and agitated for an hour. To eliminate the residual potassium permanganate, 5 mL of hydrogen peroxide was gradually added to the reaction mixture and then sterilized for 30 min. Deionized water was then added to the reaction mixture till neutrality was achieved, and then it was centrifuged to remove the precipitation. Further, the precipitate is kept at 120 °C for 5 h in an oven to obtain graphene oxide powder.

2.3. Aqueous Preparation from *C. reticulata* Peel. The 100 g *C. reticulata* peel was cleaned twice with deionized water before being cut into little pieces. The peels were dried in an N_2 environment at 55 °C for 3 days. The extract was prepared in a Soxhlet apparatus by dissolving dried peel in distilled water and gently heating it with magnetic stirring. Then, the solution cools down to room temperature, and it is filtered through filter paper to get the peel extract from *c. reticulata*.

2.4. Reduced Graphene Oxide Synthesis by Aqueous *C. reticulata* Peel. The 0.8 mol of GO powder is sonicated with 5 mol of ethanol for half hour. Then, to this reaction mixture 50 mL of aqueous *C. reticulata* peel extract is added to disperse GO, and the mixture undergoes reflux process at 90 °C for 4 h. At the end of 4th h, the color of the solution changes to black signifying the reduction of GO. This entire

https://doi.org/10.1021/acsomega.2c03446
ACS Omega 2022, 7, 40815−40825

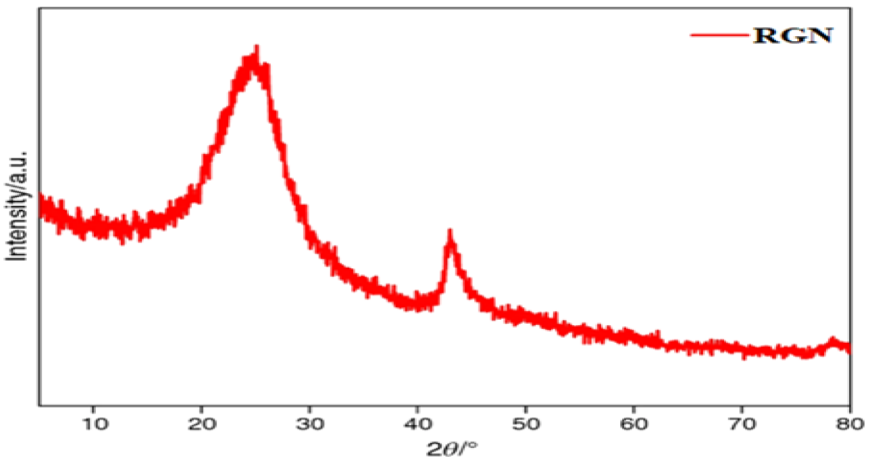

Figure 3. X-ray diffraction pattern of RGN.

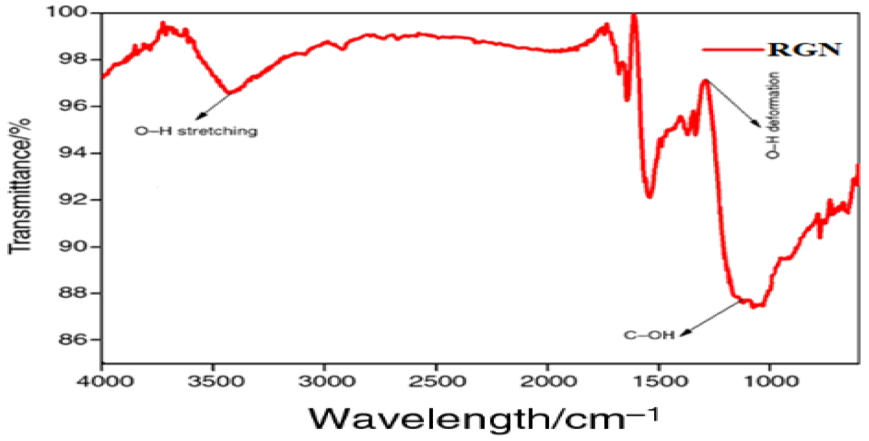

Figure 4. Fourier transform infrared spectroscopy image of RGN.

synthesis procedure was conducted at the Advanced Bioenergy and Biofuels Research Lab, Department of Energy Science and Technology, Periyar University. Synthesis process of RGN is shown in Figure 2.

2.5. Characterization of RGN. X-ray diffraction (XRD), Fourier transform infrared spectroscopy (FTIR), and scanning electron microscopy (SEM) were used to characterize the RGN. Figure 3 shows the XRD pattern of RGN. Diffraction peaks at $2\theta = 23.67°$ and $2\theta = 43.52°$ confirm the presence of RGN. The lattice spacing determined using the formula $d = \frac{n\lambda}{2 \sin \theta}$ is 0.0341 nm. Figure 4 shows FT-IR spectroscopy. The flake surface shows C−OH at 1147 cm^{-1}, O−H deformation at 1427 cm^{-1}, and O−H stretching at 3417 cm^{-1}. The morphology of the surface analyzed using SEM is displayed in Figure 5. The figure shows the size of the flake at 0.1 μm thickness. The XRD, FT-IR, and SEM images of the obtained sample confirms the presence of RGN.

2.6. Test Fuel Preparation. For the present research work, the reduced graphene oxide was prepared from agro waste areca nutshell using extracts from *C. reticulata* peel. Then, diesel is blended with isopropanol at 10 and 20% along with areca nutshell RGN at 25 ppm of RGN. The important physiognomies of the fuel mixtures are illustrated in Table 1.

2.7. Uncertainty Analysis. Factors, including visual observation, testing, environment, calibration devices, selection, and more, were taken into account while calculating experimental errors and uncertainties. The current measurement was carried out using an analytical approach, and the uncertainty was split into random and fixed errors. The measured uncertainty parameters are shown in Table 3, and the uncertainty value of different experimental devices is shown in Table 2. According to the Gaussian distribution depicted in eq 1, "T" is the estimated magnitude of uncertainty for the

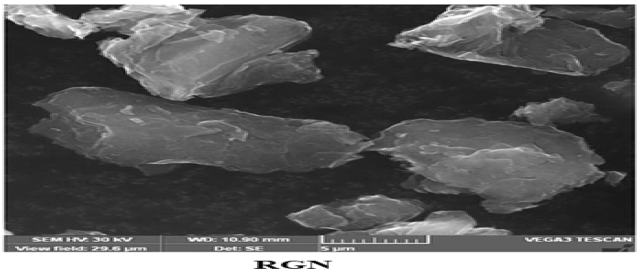

Figure 5. Scanning electron microscopy image of RGN.

Table 1. Main Properties of Blending Stocks

properties	diesel	IDR10	IDR20
density at 15 °C, kg/m^3	825.21	821.32	817.51
kinematic viscosity at 40 °C, m^2/s	3.24	2.715	2.623
calorific value, MJ/kg	46.82	44.912	43.529
cetane number	48	50	52.5
flash point	58	55	33
fire point	62	65	37

https://doi.org/10.1021/acsomega.2c03446
ACS Omega 2022, 7, 40815−40825

Table 2. Uncertainty Value of Various Experimental Instruments[9]

experimental instruments	uncertainty percentage
tachometer	0.39
smoke meter	1.28
manometer	1.6
stopwatch	0.3
exhaust gas temperature	0.16
pressure transducer	1.28
thermocouple	0.16
speed sensor	1.1

current study.[9] The below equation TP—readings,—experimental readings, and—standard deviation of the experiment could be evaluated.

$$\Delta TP = \frac{2\sigma P}{TP} \times 100\% \quad (1)$$

$$J = f(T_1, T_2, T_3, T_4, \ldots, T_n) \quad (2)$$

The above eq 2 is used for uncertainties of estimated parameters and J-function from T_1 to T_n (total number of readings).

$$\Delta J = \left(\left[\frac{\partial J}{\partial T_1} \Delta T_1 \right]^2 + \left[\frac{\partial J}{\partial T_2} \Delta T_2 \right]^2 + \left[\frac{\partial J}{\partial T_3} \Delta T_3 \right]^2 + \left[\frac{\partial J}{\partial T_4} \Delta T_4 \right]^2 + \ldots + \left[\frac{\partial J}{\partial T_n} \Delta T_n \right]^2 \right)^{1/2} \quad (3)$$

From the above eq 3, J-estimated by the root mean square of errors with measured experimental parameters, and it is further used to measure the various uncertainty parameters in Table 3.

Table 3. Uncertainty Parameters of the Experiment[9]

parameters of the experiment	uncertainty percentage
brake power	0.24
load	0.45
fuel flow rate	0.73
air flow rate	0.60
hydro carbon	0.41
carbon monoxide	0.11
time	0.79
temperature	1.49
brake specific energy consumption	0.19
smoke opacity	0.69
oxides of nitrogen	0.19

The total uncertainty of the experimental research work was estimated as follows

$$\begin{aligned} \text{total uncertainty} &= (NO_x)^2 + (CO)^2 + (THC)^2 \\ &\quad + (CO_2)^2 + (\text{smokeintensity})^2 \\ &\quad + (BTE)^2 + (EGT)^2 + (BSFC)^2 \\ &\quad + (\text{cylinder pressure})^2 \\ &= 1.47\% \end{aligned} \quad (4)$$

3. ENGINE TESTS

Figure 6 details the test engine's specs. A data acquisition system is attached to an engine to measure heat release rate (HRR), SOC, CD, ID, and mass burned within a combustion chamber. An eddy current dynamometer is also connected to an engine. The exhaust gas temperatures (EGT) are monitored by placing thermocouples in different locations. Nitrous oxide, hydrocarbon, carbon monoxide, and oxygen concentration in exhaust gas are all monitored using an AVL five-gas analyzer. K-type thermocouples were installed in a variety of places to monitor EGT. Smoke opacity is measured with a smoke meter. Measurements are done at various loads of 25, 50, 75, and 100%, respectively. Three measurements are used to arrive at these results, which are then shown on a graph.

3.1. EGR Setup. Lowering the intake charge and peak cylinder temperature increase by using an EGR system with external cooling reduced NO_x generation. Because of the increased inert gas density and increased heat capacity due to this usual cooling, a greater percentage of EGR may be employed. In order to react with fresh air from an air box, a little quantity of exhaust gas is entertained in an EGR cooler before being supplied to the manifold. Engine exhaust is hotter than intake air charge, while EGR is cooler. Exhaust gases were cooled to below 35 °C in this investigation. Recirculated exhaust and new intake charge are more effectively mixed when a mixing chamber is included with an EGR valve for managing the EGR ratio. The orifice measures exhaust flow rate. The EGR amount was calculated using eq 5.

$$\text{EGR}\ (\%) = \left(\frac{CO_2\ \text{intake}}{CO_2\ \text{exhaust}} \right) \times 100 \quad (5)$$

An MRU analyzer (which measures the amount of CO_2 at exhaust) and an EGR control valve may be used to do this (to vary the flow rate). Comparable methods for determining EGR rates were used for engines with similar specs.[16]

4. RESULTS AND DISCUSSION

4.1. Performance and Combustion Analysis. *4.1.1. Cylinder Pressure.* Peak cylinder pressure in compression ignition engines is dictated by the pace of combustion in the early phases, which is regulated by the quantity of fuel present during the delay period. As seen in Figure 7, cylinder pressure shifts in response to changes in crank angle while the engine is under full load. IDR20 has a maximum cylinder pressure of 64.80 bar, followed by IDR10 (62.13 bar), diesel (60.61 bar), EGR20−IDR10 (56.70 bar), and EGR20−IDR20 (58.80 bar), respectively. IDR20 has the highest cylinder pressure because it combines isopropanol and RGN 25 ppm with diesel, which increases cylinder pressure due to the mixture's reduced viscosity, shorter ignition delay, thermal conductivity, and greater surface to volume ratio of RGN. The oxygenated qualities of isopropanol and RGN facilitate fuel mixing and atomization, resulting in increasing cylinder pressure as the percentage of isopropanol in the blend increases. Incorporating EGR reduces cylinder pressure. This is due to the recirculation of inert gases, which function as a heat-absorbing medium, decreasing the peak pressure by lowering the cylinder's flame temperature during combustion.[17]

4.1.2. Heat Release Rate. Figure 8 depicts the changes in HRR with various IDR mixtures at full load. A variety of variables influence PCP performance, including cylinder temperature, fuel−air mixing time, and fuel characteristics.

https://doi.org/10.1021/acsomega.2c03446
ACS Omega 2022, 7, 40815−40825

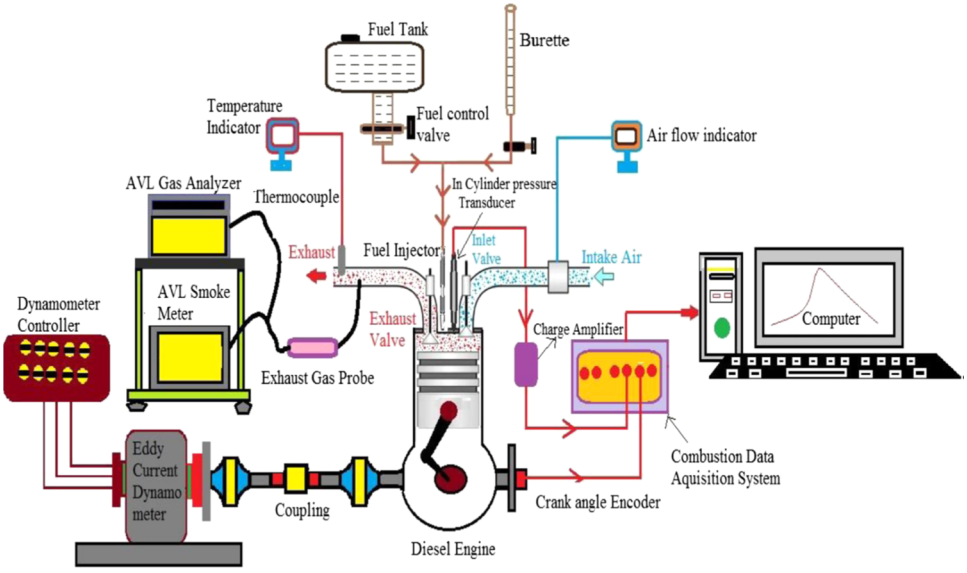

Figure 6. Test engine reprinted (adapted or reprinted in part) with permission from ref 28. Copyright [2020] [Springer].

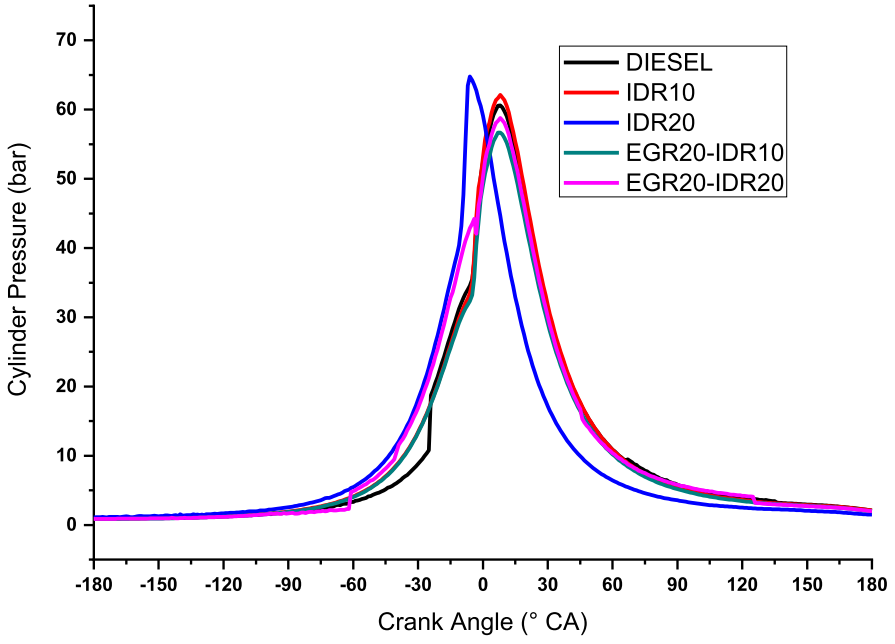

Figure 7. Disparity of cylinder pressure with IDR blends at full load.

As the combustion process proceeds, HRR begins to deviate from TDC. At full load, diesel has an HRR of 61.87 J/°CA at −2°CA, IDR10 has an HRR of 60.66 J/°CA at −3°CA, IDR20 has an HRR of 55.60 J/°CA at −4°CA, EGR20−IDR10 has an HRR of 49.75 J/°CA at −2°CA, and EGR20−IDR20 has an HRR of 44.68 J/°CA at −2°CA. According to experimental results, adding isopropanol and RGN to diesel reduces the HRR due to the fuel's shorter ignition delay and reduced calorific value. Peak HRR decreases as EGR percentages increase. This might be because the residual gases' O_2 concentration has reduced as CO_2 has been introduced to replace it. As a result, the delay time increases, allowing oxygen and fuel more time to react in situ, perhaps increasing the total quantity of the fuel in the premixed condition. Reduced oxygen concentration reduces the intensity of premixed combustion, which compensates for the lurch generated by a larger fraction of premixed fuel[18]

4.1.3. Brake Specific Fuel Consumption. For IDR mixes, Figure 9 demonstrates how brake specific fuel consumption (BSFC) varies with brake power. At all loads, IDR mixtures have a higher BSFC than diesel. This is because the blends of isopropanol and RGN with diesel have physical qualities that are relatively inferior to mineral diesel, resulting in higher fuel consumption compared to diesel at the same loading situation. Diesel has a BSFC of 0.49091 (kg/kW h) at part load, whereas the BSFC for IDR10 is 0.52148 (kg/kW h), IDR20 is 0.56682 (kg/kW h), EGR20−IDR10 is 0.65455 (kg/kW h), and EGR20−IDR20 is 0.78545 (kg/kW h). When compared to diesel, the BSFC of blends increased by 4.95% for IDR10, 11.37% for IDR20, 15.19% for EGR20−IDR10, and 25.46% for EGR20−IDR20 at full load. Though this is high compared

https://doi.org/10.1021/acsomega.2c03446
ACS Omega 2022, 7, 40815−40825

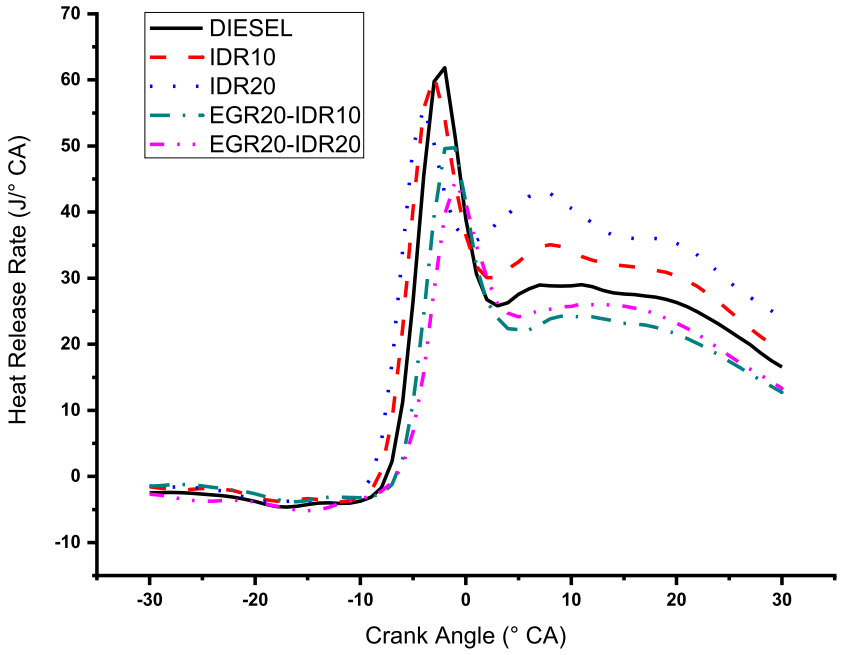

Figure 8. Disparity of HRR with IDR blends at full load.

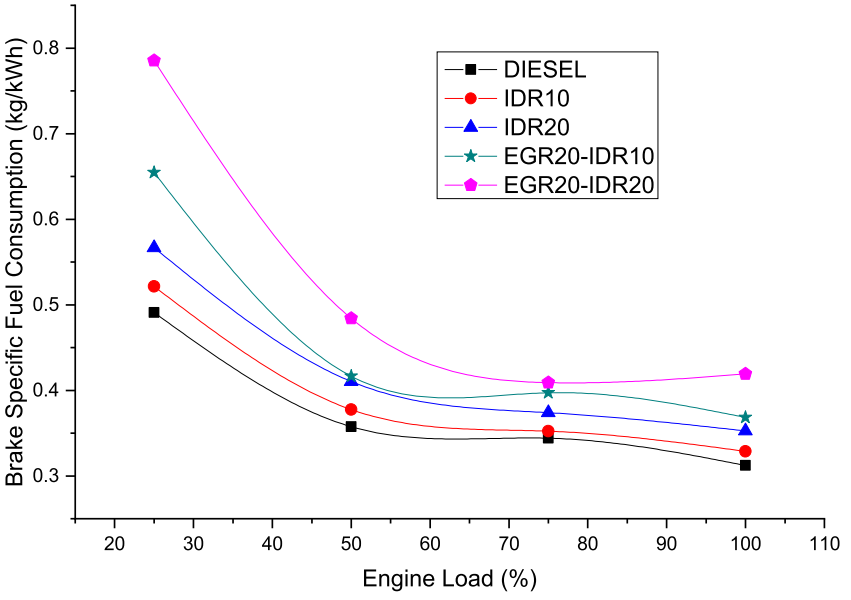

Figure 9. Disparity of BSFC with load for IDR blends.

to diesel, this consumption is minimized with a surface-to-volume ratio of nanoemulsion blends that aid in increasing the heat-transfer coefficient. Secondary atomization of water droplets present in these emulsions aids in attaining smaller droplets and speeding up evaporation rate, resulting in the effective utilization of the fuel nearly equivalent to mineral diesel. Isopropanol improves oxidation rates, which in turn reduces fuel usage compared to when EGR is introduced. The fuel consumption is even higher when the exhaust gas is recirculated into the intake valve. Because the new air is diluted by burned-out gases, more fuel is needed to maintain combustion quality.[19]

4.1.4. Brake Thermal Efficiency. Effective conversion of fuel's chemical energy into practical work is reflected in the brake thermal efficiency (BTE) of the diesel engine. Figure 10 shows the change in BTE for diesel fuel and IDR-diesel blends at various engine loads. Increasing the load results in a considerable increase in BTE due to the enhanced combustion as a result of the decreased ignition delay, increased in-cylinder temperature, and adequate timeframe for full combustion. At part load, the BTE of diesel is 19.01%, IDR10 is 18.02%, IDR20 is 16.47%, EGR20−IDR10 is 15.1%, and EGR20−IDR20 is 13.43%. In terms of BTE at full load, EGR20−IDR20, EGR20−IDR10, IDR20, and IDR10 had BTEs that were 24.08, 16.11, 11.56, and 3.76% lower than diesel. Diesel fuel, with its greater calorific value, was found to be the most efficient of the fuel mixes tested. Owing to the RGN's improved catalytic properties, which promote fuel−air mixing and combustion, the BTE of a diesel blend with isopropanol is nearly comparable to diesel, once RGN is added. All blends of

https://doi.org/10.1021/acsomega.2c03446
ACS Omega 2022, 7, 40815−40825

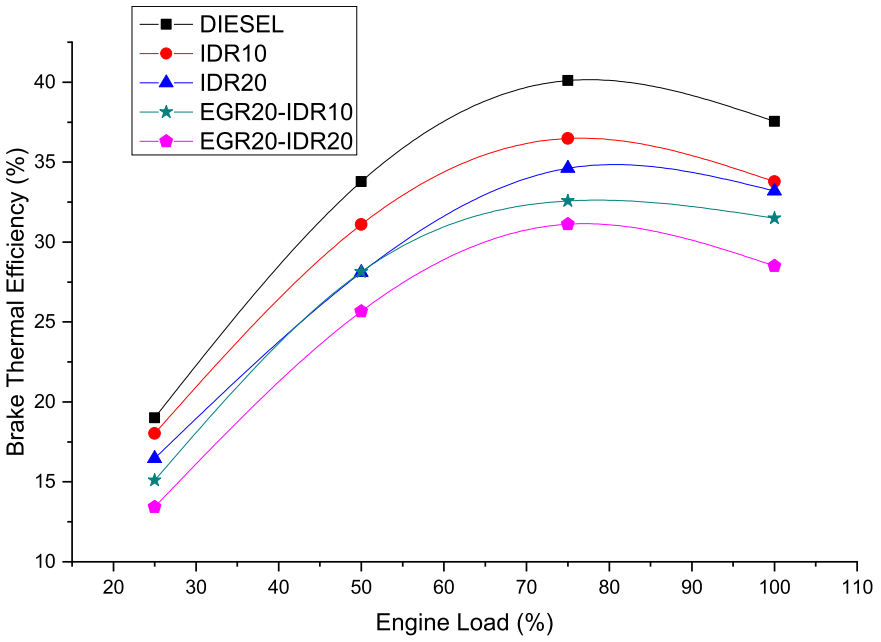

Figure 10. BTE with load for IDR blends.

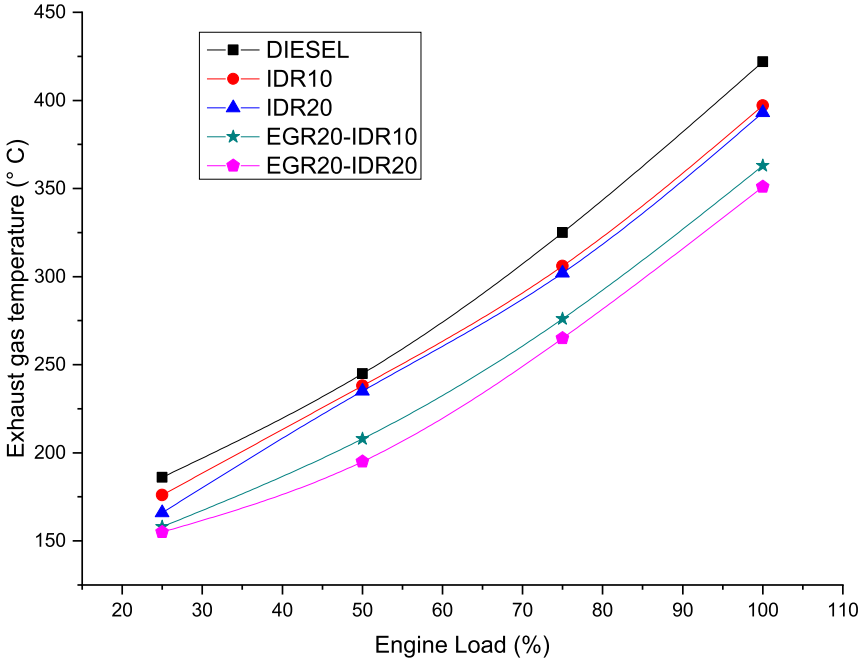

Figure 11. EGT with load for IDR blends.

plain isopropanol and RGN nanoadditives without EGR had a greater BTE than IDR blends with EGR. The three foremost effects of EGR that contribute to lower BTE levels are as follows: (1) enhanced specific thermal capacity induced by exhaust gases; (2) oxygen depletion as a result of oxygen replenishment; and (3) inadequate combustion quality due to CO_2 and H_2O in exhaust gas being chemically uncoupled.[20]

4.1.5. Exhaust Gas Temperature. Emissions from internal combustion engines are influenced by the EGT, which is a measure of how much heat is generated during combustion.[21] The exhaust gas temperature provides further information on the efficiency of the engine, the air-to-fuel ratio, the temperature produced by diffusion combustion, and the amount of oxygen that is present. Figure 11 shows that when the concentration of isopropanol increases, EGT decreases. It is because isopropanol has the lowest cetane number, the longest delay time, and the greatest cooling impact due to its greater latent heat of vaporization. At partial load, the EGT of diesel is 186 °C, IDR10 is 176 °C, IDR20 is 166 °C, EGR20−IDR10 is 158 °C, and EGR20−IDR20 is 155 °C. At full load conditions, the EGT of blends shows a depreciation of 5.92% for IDR10, 6.87% for IDR20, 13.98% for EGR20−IDR10, and 16.82% for EGR20−IDR20. Further, there is evidence to suggest that adding EGR reduces EGT. This is because higher levels of EGR dilute the residual gases,

https://doi.org/10.1021/acsomega.2c03446
ACS Omega 2022, 7, 40815−40825

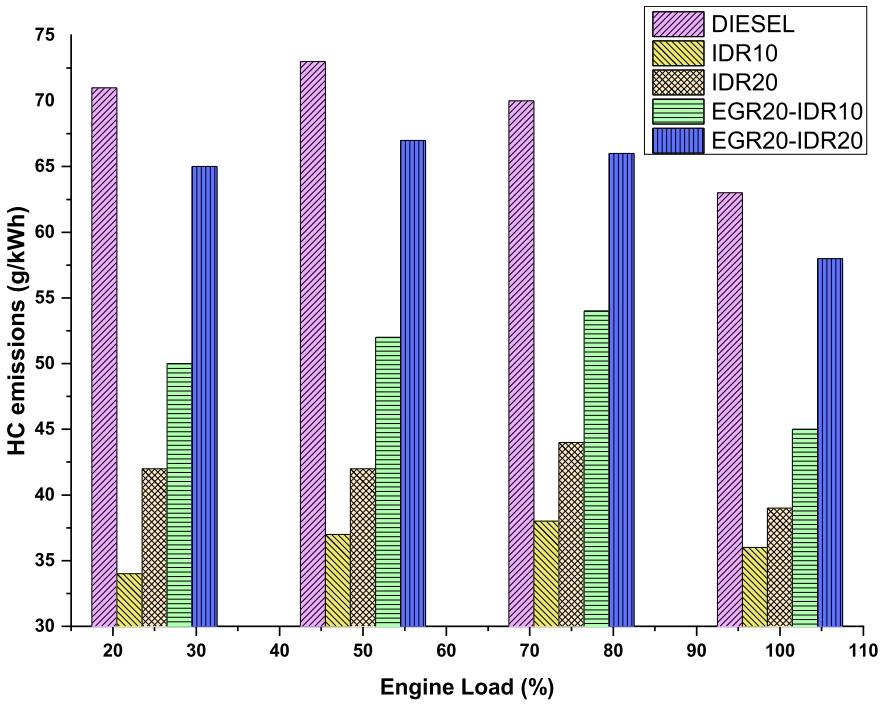

Figure 12. Disparity of hydrocarbon emission with a load for IDR blends.

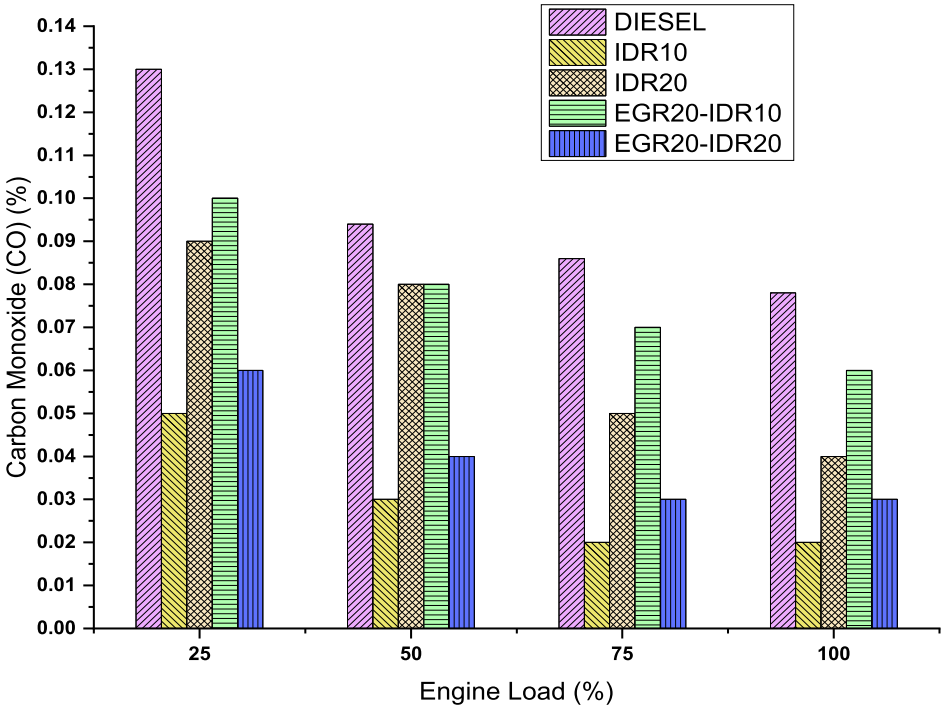

Figure 13. Disparity carbon monoxide with load for IDR blends.

decreasing the peak combustion temperature and hence reducing the temperature.[22]

4.2. Emission Analysis. *4.2.1. Hydrocarbon.* The quantity of hydrocarbons (HCs) released into an atmosphere is a good indicator of the efficiency of the combustion process. Depending on how completely the fuel was burnt, HC might be in either gaseous or solid form. Unburned hydrocarbons (HCs) are the primary source of HC emissions and may form in a variety of locations in CI engines, including those of the nozzle, crevice areas, increased aerosol impingement, and cylinder piston contact. From Figure 12, we can infer that, for all the IDR blends, the HC emissions were comparatively lower than diesel at all loads. At part load, the HC emission of diesel is 71 g/kW h, IDR10 is 34 g/kW h, IDR20 is 42 g/kW h, EGR20−IDR10 is 50 g/kW h, and EGR20−IDR20 is 65 g/kW h. This reduction in HC emissions is due to isopropanol's surplus O_2, making a leaner mixture and causing enhanced combustion compared to other fuels. At full load, HC emissions of IDR10, IDR20, EGR20−IDR10, and EGR20−IDR20 decrease by 42.85, 38.09, 28.51, and 7.93%,

https://doi.org/10.1021/acsomega.2c03446
ACS Omega 2022, 7, 40815−40825

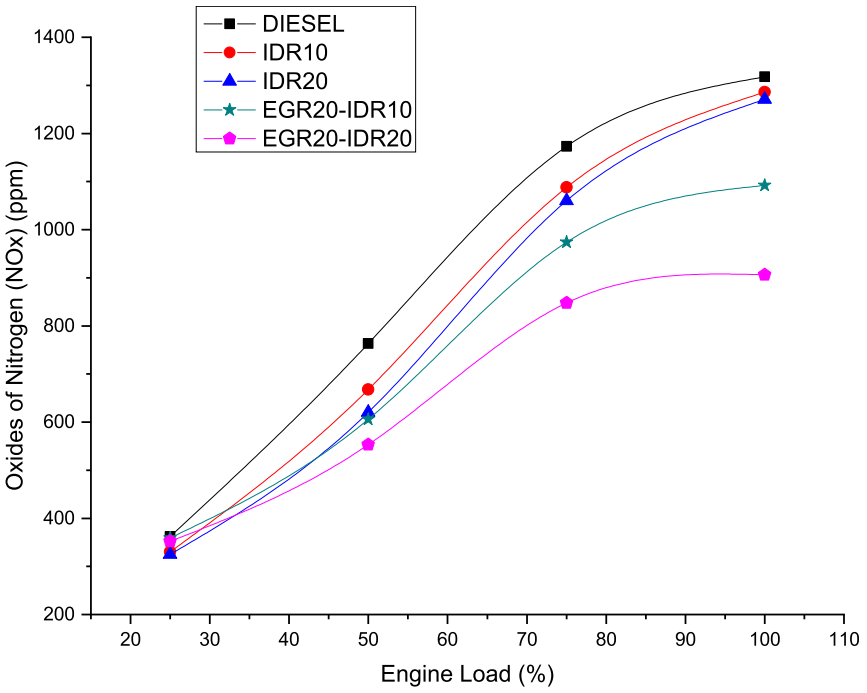

Figure 14. Disparity of nitrogen oxide emission with load for IDR blends.

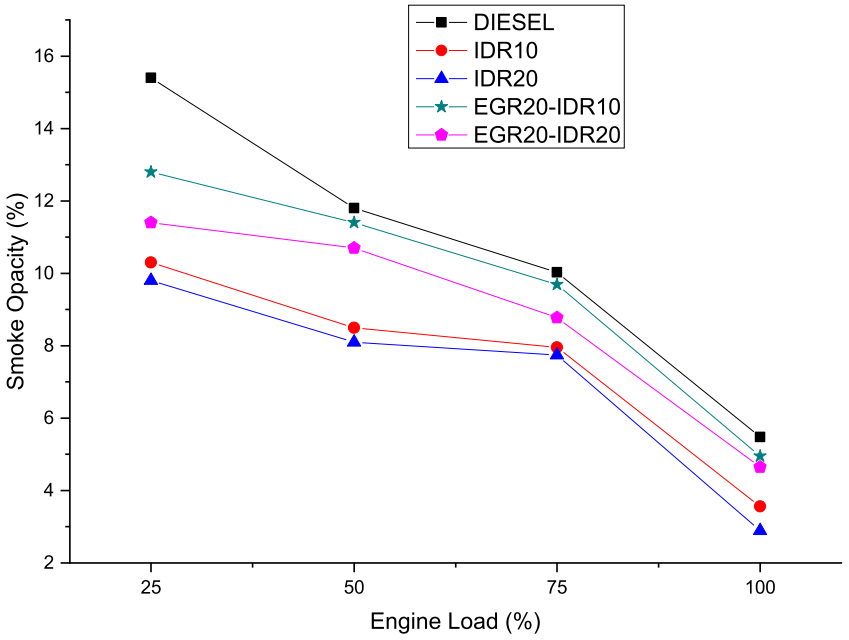

Figure 15. Disparity of smoke opacity at various engine loads for diesel and IDR blends.

respectively, when compared to diesel. This reduction in HC emissions is due to isopropanol's surplus O_2, making a leaner mixture and causing enhanced combustion. A drop in the oxidation rate due to a decrease in the intake of oxygen results in a partial oxidation and a rise in HC emissions when the fraction of EGR is increased. When you look at how rising HC emissions and falling oxygen levels go together, EGR makes more sense.[23]

4.2.2. Carbon Monoxide. In the combustion process, carbon from the fuel is converted into carbon monoxide and carbon dioxide. Oxygen deprivation causes incomplete combustion, which in turn produces more CO. Figure 13 shows the CO fluctuation for diesel IDR blends at varying engine loads. Due to greater cylinder temperatures at higher loads, CO emissions may be seen to decrease with an increase in engine load. CO emissions were 32.33% lower in all IDR blends than in diesel. This may be because the mineral diesel does not include any molecules of oxygen, which slows down the transition of carbon monoxide into carbon dioxide. As a result of the enhanced O_2 concentration, the fuel−air mixing rates are improved. The lower stoichiometric a/f ratio of IDR blends leads to a leaner operation, which results in a considerable reduction in CO emissions. IDR10 emits 0.024 ppm of CO at full load, which is less when EGR is introduced. This is the result of the combustion process degrading due to the reduced O_2 concentration that EGR provides.[24]

https://doi.org/10.1021/acsomega.2c03446
ACS Omega 2022, 7, 40815−40825

4.2.3. Oxides of Nitrogen (NO_x). Increased temperatures within a chamber are primarily responsible for the emission of NO_x. Nitrogen and oxygen combine to generate nitrogen oxide when subjected to very high temperatures. Figure 14 shows the NO_x variation at various engine loads for diesel and IDR blends. Compared to diesel, NO_x emitted by the IDR blends is lower. At partial load, NO_x emission of diesel is 362 ppm, IDR10 is 330 ppm, IDR20 is 325 ppm, EGR20−IDR10 is 359 ppm, and EGR30−ISP30 is 352 ppm. The cooling effect of isopropanol (due to its high latent heat, low boiling point, and lower calorific value) reduces NO_x emissions as the concentration of isopropanol in diesel increases.[25] This is contrary to the general belief that higher cylinder temperatures occur with lower cetane rating. At 100% load, emission of NO_x is reduced by 2.42% for IDR10, 3.57% for IDR20, 17.15% for EGR20−IDR10, and 31.26% for EGR20−IDR20, respectively, compared to diesel. As the EGR concentration rises, the cylinder's O_2 concentration drops and the flame propagation temperature drops, which in turn decreases NO_x emissions. High temperatures in the cylinder chamber are inevitably affected by the overall heat capacity of the working gas, which, in turn, decreases dramatically as the EGR percentage increases. With lower peak cylinder temperatures and less NO_x production, IDR blends are more environmentally friendly.[26]

4.2.4. Smoke Opacity. In order to generate smoke, engines shatter the fuel's components into atomic grains, which are then oxidized in the reaction chamber. Excessive fuel accumulation, reduced atomization, and higher C/H ratios in the fuel all play a role in the production of smoke. Figure 15 shows the variation of smoke opacity at various engine loads for diesel and IDR blends. With increasing isopropanol concentration in blends, there is a reduction in smoke opacity. At partial load, smoke formation of diesel is 15.4%, IDR10 is 10.3%, IDR20 is 9.8%, EGR20−IDR10 is 12.8%, and EGR20−IDR20 is 11.4%. This is because alcohols include inherent oxygen that aids burning, decreasing the fuel-rich zones, enhancing mixing rates, and reducing the risk of soot formation, particularly during the diffusion combustion phase. At 100% load, the smoke formation decreases for IDR10 by 35.04%, for IDR20 by 47.26%, EGR20−IDR10 by 9.67%, and EGR20−IDR20 by 15.15% compared to diesel. Increasing the EGR percentage results in the rise of smoke opacity. It is a consequence of unstable combustion caused by exhaust gases replacing some of the air in the combustion process.[27]

5. CONCLUSIONS

During this current study, the impact of IDR addition with fuel on engine performance and emissions with EGR was investigated and compared with fuel. Based on the experimental results, the subsequent conclusions were drawn

1. Isopropyl alcohol is added to diesel with no changes to the engine because there have been no phase separations for 96 h.
2. IDR10 consumes 4.95% more fuel and has a 3.76% lower BTE compared to diesel. Though this is marginally elevated compared to diesel, this consumption is minimized compared with conventional biodiesel because of the surface-to-volume ratio of nanoemulsion blends that aid in increasing the heat-transfer coefficient and secondary atomization of water droplets present in these emulsions aids in attaining smaller droplets and speeding up evaporation rate, resulting in effective utilization of the fuel
3. Compared to diesel, IDR10 exhibits 23% higher HRR. Adding isopropanol and RGN to diesel reduces the HRR due to the fuel's shorter ignition delay and reduced calorific value. Peak HRR decreases as EGR percentages increase. This might be because the residual gases' O_2 concentration has reduced as CO_2 has been introduced to replace it.
4. The IDR blends with 25 ppm RGN, 10% isopropanol, and 90% diesel show reduced emissions of HC by 42.85%, CO by 33.34%, NO_x by 2.42%, and smoke by 15.4%, compared to mineral diesel due to isopropanol's surplus O_2, improved the fuel−air mixing rates causing enhanced combustion.

From the experimental results, it is concluded that though the introduction of EGR along with IDR blends reduces NO_x, the other parameters of emission and performance characteristics of the fuel blend with 25 ppm RGN, 10% isopropanol, and 90% diesel are superior and can be an immediate alternate to mineral diesel in IC engines.

AUTHOR INFORMATION

Corresponding Author

Ganapathi Arumugam − *Department of Energy Science and Technology, Periyar University, Salem 636011, India;* orcid.org/0000-0002-3692-3822; Phone: +91-8807718858; Email: ganomec@gmail.com

Authors

Kandasamy Muralidharan − *Department of Mechanical Engineering, Sona College of Technology, Salem 636005, India*

Amjad A. Pasha − *Aerospace Engineering Department, King Abdulaziz University, Jeddah 21589, Saudi Arabia*

Nazrul Islam − *Department of Mechanical Engineering, King Abdulaziz University, Jeddah 21589, Saudi Arabia*

Complete contact information is available at: https://pubs.acs.org/10.1021/acsomega.2c03446

Notes

The authors declare no competing financial interest.

ACKNOWLEDGMENTS

The authors gratefully acknowledge the technical support provided by the Deanship of Scientific Research (DSR), King Abdulaziz University, Jeddah.

ABBREVIATIONS

BSU	Bosch smoke unit
BSFC	brake specific fuel consumption
CO	carbon monoxide
DAS	data acquisition system
EGR	exhaust gas recirculation
EGT	exhaust gas temperature
HC	hydrocarbon
CP	cylinder pressure
ID	ignition delay
HRR	heat release rate
ISP	isopropanol (isopropyl alcohol)
RGN	reduced graphene oxide

https://doi.org/10.1021/acsomega.2c03446
ACS Omega 2022, 7, 40815−40825

IDR10	10% isopropanol + 80% diesel fuel + 25 ppm RGN
IDR20	20% isopropanol + 80% diesel fuel + 25 ppm RGN
EGR20−10IDR	20%EGR + IDR10
EGR20−20IDR	20%EGR + IDR20
SOC	start of combustion

REFERENCES

(1) Arya, M.; Kumar Rout, A.; Samanta, S. A Review onThe Effect Of Engine Performance And Emission Characteristics Of C.I. Engine Using Diesel-Biodiesel-Additives Fuel Blend. *Mater. Today: Proc.* **2022**, *51*, 2224−2232.

(2) Xu, L.; Wang, Y.; Liu, D. Effects Of Oxygenated Biofuel Additives On Soot Formation: A Comprehensive Review Of Laboratory-Scale Studies. *Fuel* **2022**, *313*, 122635.

(3) Sharma, N.; Patel, C.; Tiwari, N.; Agarwal, A. Experimental Investigations Of Noise And Vibration Characteristics Of Gasoline-Methanol Blend Fuelled Gasoline Direct Injection Engine And Their Relationship With Combustion Characteristics. *Appl. Therm. Eng.* **2019**, *158*, 113754.

(4) Kocakulak, T.; Babagiray, M.; Nacak, Ç.; Safieddin Ardebili, S.; Calam, A.; Solmaz, H. Multi Objective Optimization Of HCCI Combustion Fuelled With Fusel Oil And N-Heptane Blends. *Renew. Energy* **2022**, *182*, 827−841.

(5) Fan, Y.; Zhang, J.; Zhang, Q.; Ma, X.; Liu, Z.; Lu, M.; Qiao, K.; Li, F. Biofuel And Chemical Production From Carbon One Industry Flux Gas By Acetogenic Bacteria. *Adv. Appl. Microbiol.* **2021**, *117*, 1−34.

(6) Tuan Hoang, A.; Xuan Le, M.; Nižetić, S.; Huang, Z.; Ağbulut, Ü.; Veza, I.; Said, Z.; Tuan Le, A.; Dung Tran, V.; Phuong Nguyen, X. Understanding Behaviors Of Compression Ignition Engine Running On Metal Nanoparticle Additives-Included Fuels: A Control Comparison Between Biodiesel And Diesel Fuel. *Fuel* **2022**, *326*, 124981.

(7) Hosseini, S.; Taghizadeh-Alisaraei, A.; Ghobadian, B.; Abbaszadeh-Mayvan, A. Performance And Emission Characteristics Of A CI Engine Fuelled With Carbon Nanotubes And Diesel-Biodiesel Blends. *Renew. Energy* **2017**, *111*, 201−213.

(8) Sathiyamoorthi, R.; Sankaranarayanan, G. The Effects Of Using Ethanol As Additive On The Combustion And Emissions Of A Direct Injection Diesel Engine Fuelled With Neat Lemongrass Oil-Diesel Fuel Blend. *Renew. Energy* **2017**, *101*, 747−756.

(9) Arumugam, G.; Muralidharan, K. Influence of Biodegradable Graphene Oxide Nano-Platelets Blended With Indian Geranium Grass Biodiesel In A Diesel Engine. *Int. J. Environ. Sci. Technol.* **2021**, *19*, 8613−8632.

(10) Raju, V.; Venu, H.; Subramani, L.; Reddy, S.Comparative Assessment Of Various Nanoadditives On The Characteristic Diesel Engine Powered By Novel Tamarind Seed-Methyl Ester Blend. *Recent Technologies for Enhancing Performance and Reducing Emissions in Diesel Engines*; IGI Global, 2020; pp 138−158.

(11) Öztürk, E.; Can, Ö. Effects Of EGR, Injection Retardation And Ethanol Addition On Combustion, Performance And Emissions Of A DI Diesel Engine Fueled With Canola Biodiesel/Diesel Fuel Blend. *Energy* **2022**, *244*, 123129.

(12) Sogbesan, O.; Garner, C.; Davy, M. The Effects of Increasing FAME Biodiesel Content On Combustion Characteristics And HC Emissions In High-EGR Low Temperature Combustion. *Fuel* **2021**, *302*, 121055.

(13) Dubey, A.; Prasad, R.; Kumar Singh, J.; Nayyar, A. Optimization Of Diesel Engine Performance And Emissions With Biodiesel-Diesel Blends And EGR Using Response Surface Methodology (RSM). *Clean. Eng. Technol.* **2022**, *8*, 100509.

(14) Bardhan, M.; Novera, T.; Tabassum, M.; Islam, M.; Jawad, A.; Islam, M. Adsorption Of Methylene Blue Onto Betel Nut Husk-Based Activated Carbon Prepared By Sodium Hydroxide Activation Process. *Water Sci. Technol.* **2020**, *82*, 1932−1949.

(15) Ituen, E.; Ekemini, E.; Yuanhua, L.; Singh, A. Green Synthesis Of Citrus Reticulata Peels Extract Silver Nanoparticles And Characterization Of Structural, Biocide And Anticorrosion Properties. *J. Mol. Struct.* **2020**, *1207*, 127819.

(16) Venu, H.; Subramani, L.; Raju, V. Emission Reduction In A DI Diesel Engine Using Exhaust Gas Recirculation (EGR) Of Palm Biodiesel Blended With Tio2 Nano Additives. *Renew. Energy* **2019**, *140*, 245−263.

(17) Gülüm, M. Effects Of Compression Ratio, Blending Ratio And Engine Speed On Fuel Cost, Performance And Exhaust Emissions Of A Diesel Engine Fueled With Bio-Derived Alternative Fuels. *Sustain. Energy Technol. Assessments* **2022**, *53*, 102464.

(18) Liang, J.; Zhang, Q.; Chen, Z.; Zheng, Z. The Effects of EGR Rates And Ternary Blends Of Biodiesel/N-Pentanol/Diesel On The Combustion And Emission Characteristics Of A CRDI Diesel Engine. *Fuel* **2021**, *286*, 119297.

(19) Dhanarasu, M.; RameshKumar, K. A.; Maadeswaran, P. Effect Of Acetone As An Oxygenated Additive With Used Sunflower Oil Biodiesel On Performance, Combustion And Emission In Diesel Engine. *Environ. Technol.* **2021**, *43*, 3682−3692.

(20) Gowthama Krishnan, M.; Rajkumar, S. Effects Of Start Of Injection And Exhaust Gas Recirculation On Dual Fuel Combustion Of Isobutanol With Diesel And Waste Cooking Oil Biodiesel In A Diesel Engine At Higher Loads. *Fuel* **2022**, *327*, 125097.

(21) Krishnamoorthi, M.; Malayalamurthi, R. Effect Of Exhaust Gas Recirculation And Charge Inlet Temperature On Performance, Combustion, And Emission Characteristics Of Diesel Engine With Bael Oil Blends. *Energy Environ.* **2018**, *29*, 372−391.

(22) Yaliwal, V.; Banapurmath, N.; Soudagar, M.; Afzal, A.; Ahmadi, P. Effect Of Manifold And Port Injection Of Hydrogen And Exhaust Gas Recirculation (EGR) In Dairy Scum Biodiesel - Low Energy Content Gas-Fueled CI Engine Operated On Dual Fuel Mode. *Int. J. Hydrogen Energy* **2022**, *47*, 6873−6897.

(23) Sunil Naik, N.; Balakrishna, B. Effects of EGR On Performance And Emissions Of A Diesel Engine Fuelled With BalanitesAegyptiaca/Diesel Blends. *Int. J. Sustain. Eng.* **2017**, *11*, 150−158.

(24) Chen, S.; Cui, K.; Zhu, J.; Zhao, Y.; Wang, L.; Mutuku, J. Effect of Exhaust Gas Recirculation Rate on the Emissions of Persistent Organic Pollutants from a Diesel Engine. *Aerosol Air Qual. Res.* **2019**, *19*, 812−819.

(25) Modi, A.; Gosai, D.; Solanki, C. Experimental Study of Effect of EGR Rates on NOx and Smoke Emission of LHR Diesel Engine Fueled with Blends of Diesel and Neem Biodiesel. *J. Inst. Eng. (India): Ser. C* **2017**, *99*, 181−195.

(26) Patil, V.; Thirumalini, S. Effect of cooled EGR on performance and emission characteristics of diesel engine with diesel and diesel-karanja blend. *Mater. Today: Proc.* **2021**, *46*, 4720−4727.

(27) Klajn, F.; Gurgacz, F.; Lenz, A.; Iacono, G.; Souza, S.; Ferruzzi, Y. Comparison of the emissions and performance of ethanol-added diesel−biodiesel blends in a compression ignition engine with those of pure diesel. *Environ. Technol.* **2018**, *41*, 511−520.

(28) Ganapathi, A.; Muralidharan, K. Impact of Indian Geranium Grass Biodiesel Blends on Performance, Combustion and Emission Characteristics. *Int. J. Thermophys.* **2020**, *41*, 137.

https://doi.org/10.1021/acsomega.2c03446
ACS Omega 2022, 7, 40815−40825